Journal of the European Ceramic Society 17 (1997) 439–445

PII: S0955-2219(96)00109-4
0955-2219/97/$17.00

Superplasticity of HIP $MgO{\cdot}Al_2O_3$ Spinel: Prospects for Superplastic Forming

F. Beclin,[a] R. Duclos,[a] J. Crampon[a] & F. Valin[b]

[a]Laboratoire de Structure et Propriétés de l'Etat Solide, CNRS (URA 234), Bât C6, U.S. T. Lille, 59655 Villeneuve-d'Ascq Cedex, France
[b]Centre d'Etudes de Saclay, CEN/CE2M/LECMA, 91191 Gif-sur-Yvette, France

(Received 15 September 1995; accepted 10 June 1996)

Abstract

Polycrystals of hot-isostatically pressed $MgO{\cdot}Al_2O_3$ spinel, having a fine-grained size of 610 nm, have been deformed in uniaxial compression. The results have been analysed by taking into account grain growth. The variation in stress exponent n *suggests a transition from interface reaction* (n = *2) at low stresses to diffusional mechanism* (n = *1) at high stresses, but cavitational creep was responsible for the non-linear behaviour at stresses above 60 MPa. The grain size exponent found at 60 MPa* (p = *3), the absence of dislocations within the fine grains and the similarity of equiaxed grain shapes before and after large flow (≈40%) resemble the characteristics of micrograin superplastic flow. The value of the grain size exponent suggests that grain-boundary diffusion makes a significant contribution at medium stresses to the diffusion-accommodated grain-boundary sliding. Post-HIP treatment of superplastically deformed samples results in a general density increase and improved transparency for the less stressed sample. © 1996 Elsevier Science Limited.*

Des polycristaux de spinelle $MgO{\cdot}Al_2O_3$ pressés isostatiquement à chaud, à grains très fins (610 nm), ont été déformés en compression. La croissance de grain est considérée lors de l'analyse des résultats. La variation de l'exposant de contrainte n *suggère la transition d'un mécanisme de réaction d'interface* (n = *2) aux faibles contraintes à celui de la diffusion* (n = *1) aux contraintes élevées. La cavitation conduit à un comportement non linéaire au dessus de 60 MPa. L'exposant de taille de grain obtenu à 60 MPa* (p = *3) suggère que la diffusion aux joints de grain est prépondérente. L'absence de dislocations dans les grains fins et le maintien de la forme équiaxée des grains après une déformation importante (≈40%) sont caractéristiques d'une superplasticité structurale. Un pressage isostatique à chaud ultérieur des échantillons déformés conduit à une augmentation de la densité et une amélioration de la transparence de l'échantillon déformé aux contraintes faibles.*

1 Introduction

Previous studies on ultrafine-grained ceramics have demonstrated that superplasticity could be considered as a potential option for near-net-shape forming of these ceramic systems.[1–6] Not surprisingly, increasing investigations of superplastic ceramic systems have been reported to date, and clear evidence has been provided for the phenomenon which was followed by a demonstration of shaping by superplastic forming.[3,7–9]

In the case of $MgO{\cdot}xAl_2O_3$ spinel system, which is considered as a suitable candidate for new technologies needing optical materials with good mechanical properties, efforts have been made to achieve hemispherical shapes with the best visible and i.r. transparency by practical processing. In this way, the optical quality of the sintered aluminate of magnesium has been less than that of hot-pressed spinel. Thus, although powder sintering offers the advantage of ease of obtaining hemispherical shapes, other innovative fabrication routes have also been explored. All were based initially on the plastic deformation of monocrystalline ceramics, and more recently on the flow behaviour of polycrystalline ceramics. Firstly, press-forging of Al_2O_3-rich spinel single crystals[10] ($MgO{\cdot}3Al_2O_3$) to flat discs was investigated in the processing temperature range 1650–1750°C. Following this preliminary work, press-forging of small domes of spinel[11] using $MgO{\cdot}2Al_2O_3$ single crystals as well as $MgO{\cdot}3{\cdot}5Al_2O_3$ polycrystals was studied. Good results were obtained at temperatures of 1750–1780°C and stresses of 70–105 MPa.

About 10 years ago it was demonstrated that fine-grained (<5 μm) fully dense magnesia–alumina spinel[12] ($MgO{\cdot}2Al_2O_3$) can be plastically deformed to large strains under uniaxial compression at temperatures from 1450 to 1612°C. The processing map arising from this basic work and showing the influence of strain rate and temperature on the ductility of this fine-grained $MgO{\cdot}2Al_2O_3$ spinel, has subsequently served as a guideline to produce near-net-shape forging of ceramic parts[13] in the form of a lens by sinter-forging porous preforms of such a material at 1573°C.

As stoichiometric spinel requires higher temperature and stress to activate plastic deformation, needed for press-forging, than do Al_2O_3-rich compositions,[14,15] only alumina supersaturated compositions have been used for these press-forging investigations. More recently, as a result of the development of ultrafine-grained spinel (0·5 μm grain size) by hot-pressing, superplastic deformation could be achieved at a flow stress of 80 MPa in equimolar spinel, and hemispherical domes[16] were fabricated by press-forming at 1400°C.

This brief survey on the spinel system shows that considerable efforts have been directed in the past to the development of equiaxed, very fine-grained microstructure suitable to be both sintered to full density and processed by superplastic forming. However, due to some problems encountered, such as α-Al_2O_3 precipitation in alumina supersaturated spinel,[12] platinium precipitation in $Pt/MgO{\cdot}xAl_2O_3$ nanocomposites[17] and bimodal grain-size distribution in hot-pressed equimolar spinel,[16,18] the procedures used to date for the preparation of superplastic spinel have not yet reached this goal.

As direct hot-isostatic press(HIP)ing is known to be very effective to achieve fully dense materials with very fine-grained microstructure, we have attempted to develop equimolar $MgO{\cdot}Al_2O_3$ spinel by this route. In order to test for the existence of superplasticity in this HIPed material, compressive creep tests and extensive microstructural characterization have been performed. Finally, some deformed samples have been post-HIPed to test for the possibility of healing the damage resulting from the superplastic deformation.

2 Experiments

$MgO{\cdot}Al_2O_3$ samples were hot-isostatically pressed in containers at temperatures from 1350 to 1450°C. The HIPing conditions were carefully monitored to obtain a material with minimum grain size and minimum porosity. Samples were characterized by their density measured by Archimedes' method in alcohol, the theoretical density of $MgO{\cdot}Al_2O_3$ being 3·58 g cm^{-3}. The microstructure was analysed by transmission electron microscopy (TEM).

Before creep tests, the samples were annealed in air at 1380°C in order to release the internal stresses resulting from HIPing conditions.

Compressive tests were performed in air in a creep machine working under constant stress and temperature. Compression samples having a typical size of 3 × 3 × 7 mm^3 were deformed under stresses and temperatures ranging respectively from 15 to 90 MPa and from 1350 to 1420°C. For microstructural and density comparisons each sample had a companion which was submitted to the test temperature sequence only without loading.

To test for the prospect for superplastic forming, some deformed samples were then submitted to a post-HIP treatment in order to heal the damage occurring during the creep tests.

3 Results

3.1 Temperature effects on densification

Table 1 shows the results at different HIP conditions. Above 1400°C the theoretical density should be attained, but the microstructure evolved towards a bimodal grain size with abnormal grain growth as already encountered elsewhere.[16,18] Thus polycrystals HIPed at 1400°C, showing a fine-grained microstructure of 0·51 μm grain size and having a residual porosity $(1 - \rho/\rho_{theo}) \times 100$ of 0·3%, were selected to be deformed in uniaxial compression.

3.2 Microstructural effects of deformation and post-HIP treatment

In previous work on superplastic deformation in fine-grained spinel, a transition from semi-brittle behaviour to ductile behaviour has been evidenced. As the strain rate was lowered, the material could be deformed without any evidence of surface cracks.[12] However, such a macroscopic observation is insufficient to know whether forming will be accompanied by cavity production and microstructural damage characterization by TEM is thus necessary.

Table 1. Density and grain size developments for different HIP conditions

	HIPing temperature (°C)				
	1350	*1380*	*1400*	*1410*	*1450*
Green density (g cm^{-3})	2·37	–	2·27	2·35	2·35
Final density (g cm^{-3})	3·53	3·54	3·57	3·57	3·58
Porosity (%)	1·4	1·1	0·3	0·3	0
Grain size (μm)	0·48	0·51	0·51	0·57	0·8

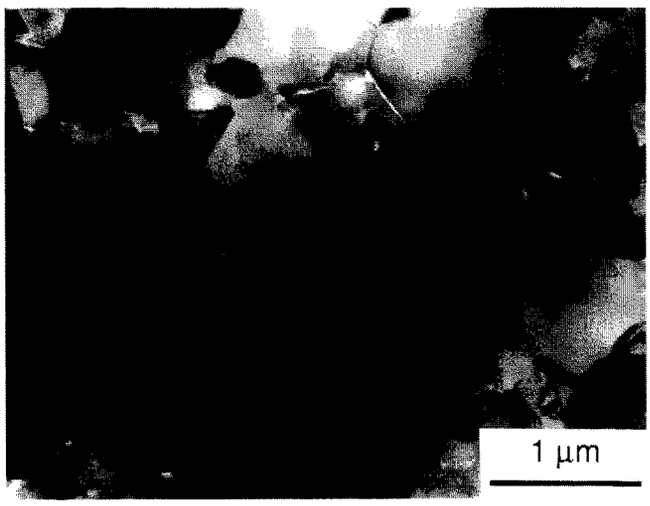

(a)

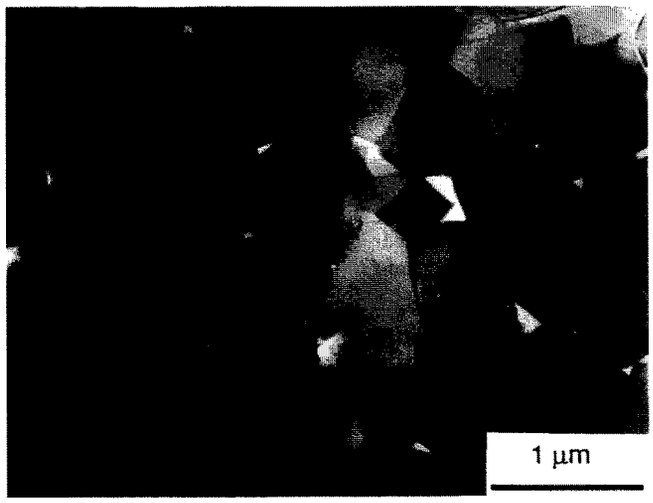

(b)

Fig. 1. Fine-grained microstructure and residual porosity of (a) as-HIPed polycrystalline $MgO{\cdot}Al_2O_3$ (T = 1400°C) and (b) annealed sample (T = 1380°C).

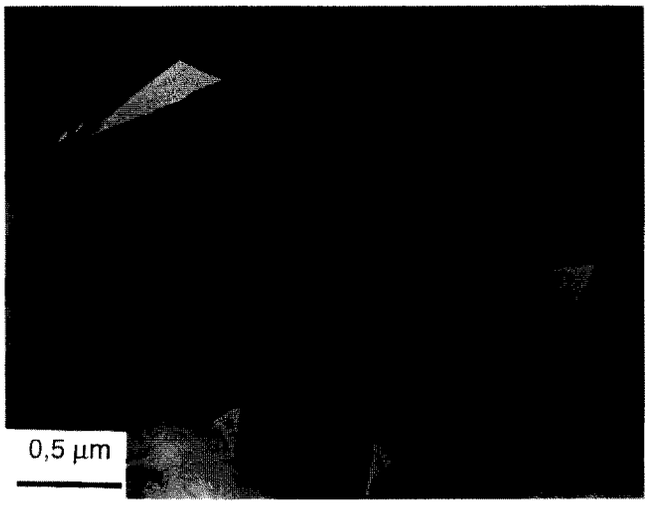

(a)

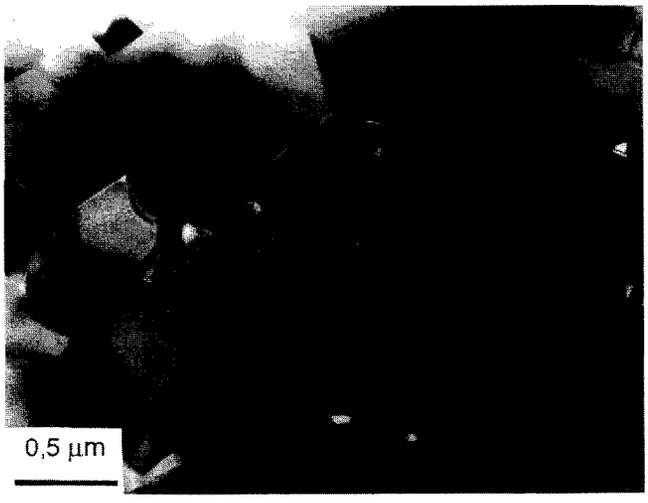

(b)

Fig. 2. (a) Lack of dislocation and grain growth in deformed sample (ε = 31%, T = 1380°C, σ = 60 MPa); (b) companion of the previous sample.

Typical fine-grained microstructures of as-HIPed and annealed samples are shown in Fig. 1. The main feature encountered was a noticeable lack of dislocation within these very fine grains. The fine intergranular porosity was the cause of the white colouring of the material.

As seen in Fig. 2, the microstructure in deformed samples was very similar to that of as-HIPed samples except for the appearance of strain-enhanced grain growth. The grains were still free of dislocation and as equiaxed as in the starting material, indicating a grain switching mechanism such as that proposed by Ashby and Verrall.[19] Although no internal microcracking was observed throughout the material, even after about 40% true strain, deformed samples presented some damage, as small cavities located at some grain-boundary triple points. In quantity, this damage was slightly more than that encountered in their annealed-only companions.

Finally, TEM observations after post-HIPing of the sample deformed at the lowest stresses show that the intergranular cavities in the fine-grained matrix practically disappeared by this treatment (Fig. 3). More generally, in the post-HIPed samples the strain-induced damage has been largely healed.

3.3 Damage evaluation

After annealing treatment the porosity increased to 1·7% and, in order to quantify the cavitation produced by superplastic deformation and healed by post-HIP treatment, the densities of the deformed and the post-HIPed samples were compared with that of the annealed-only sample. Table 2 compares the results of the total porosity (P_1 and P_3) after deformation and post-HIP treatment, $(1 - \rho/\rho_{theo}) \times 100$, with the contribution from strain-induced porosity (P_2), $(1 - \rho/\rho_{anneal}) \times 100$.

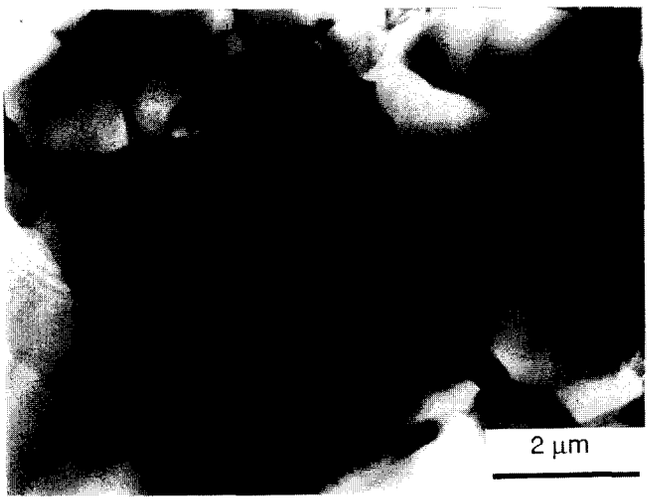

Fig. 3. Healing of the porosity in a post-HIPed sample.

Table 2. Porosity development after deformation and post-HIP treatment

T(°C)	σ (MPa)	ε (%)	P_1 (%)	P_2 (%)	P_3 (%)
1380	15–45	22·5	2	0·3	0·6
	30–60	27·4	3·6	2	2·2
	45	27	3·4	1·7	
	60	17·5	2·6	1·1	
	60	31	3·7	2	
	60	37	3·7	2	
1400	45	27	3	1·4	
	60	38	3·4	1·7	1·1
1420	60	38	3·7	2	

Results given in Table 2 show that the total porosity in the sample deformed at the lowest stresses and then post-HIPed has been reduced to the porosity level of the as-HIPed samples.

3.4 Grain growth

There is clear evidence in the data of Table 3 that grain growth occurs during the whole experiment. Furthermore, grain growth was more important for deformed samples than for annealed-only ones; thus dynamic grain growth appears to be very significant in our experiments.

3.5 Creep curves, stress and grain size dependence

3.5.1 Creep curves

At high temperature the phenomenological relationship between the stationary strain rate $\dot{\varepsilon}_S$ and the stress σ can be classically written as a Norton law:

$$\dot{\varepsilon}_S = A\sigma^n \qquad (1)$$

The stress exponent n characterizes the deformation process involved. A is a function of the microstructure, particularly the average grain size $<d>$ in the case of a diffusional mechanism,[20,21] which predicts

Table 3. Comparison of the grain size for deformed samples (at 1380°C and 60 MPa) and their annealed-only companions (at 1380°C)

	Total time		
	2 h 13 min	3 h 55 min	3 h 52 min
Total strain, ε (%)	17·5	31	37
Average grain size (µm)			
deformed samples	0·85	1	1
annealed samples	0·75	0·86	0·83
initial samples	0·61	0·61	0·51

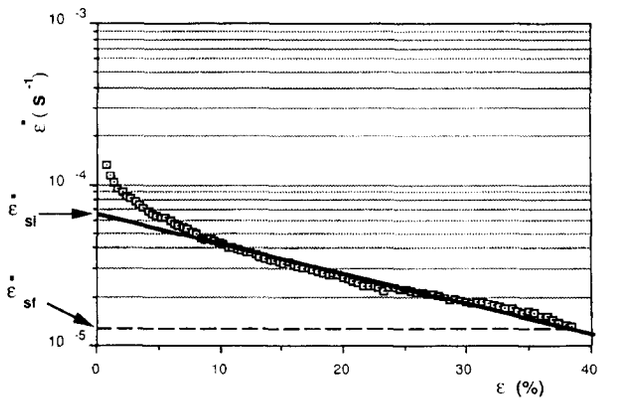

Fig. 4. Continuous linear decrease of the creep rate after a transient period (T = 1400°C, σ = 60 MPa).

that $A = A' <d>^{-p}$ where the grain size exponent p is typically 2 or 3. Equation (1) can thus be written:

$$\mathrm{Ln}\,\dot{\varepsilon}_S = \mathrm{Ln}\,A' + n \ln \sigma - p \ln <d> \qquad (2)$$

Figure 4 shows the $\ln \dot{\varepsilon}_S$ versus ε_S plot for a sample compressed at 60 MPa and 1400°C. The quasi-linear part of this curve, observed after a transient part, corresponds to pseudo-stationary creep. The continuous decrease of the creep rate $\dot{\varepsilon}_S$ reflects the strain hardening due to strain-enhanced grain growth. From the creep tests it appears that samples of fine-grained spinel of equimolar composition present a real ability to be superplastically deformed since a true strain of about 40% was easily achieved without the occurrence of any tertiary stage.

3.5.2 Stress exponent n

By using eqn (2) for the analysis of experimental data, the stress exponent n can be deduced from the dependence of $\ln \dot{\varepsilon}_S$ on σ. As shown in eqn (1), determination of the true value of n depends on the possibility of keeping a constant value for the structural parameter A. Isostructural values of n have been determined by the stress jump method as shown in Fig. 5.

Table 4, showing the results of the stress exponent n determined at 1380°C, indicates a dependence of the stress exponent n on stress. In the lowest studied stress range (15–45 MPa), the

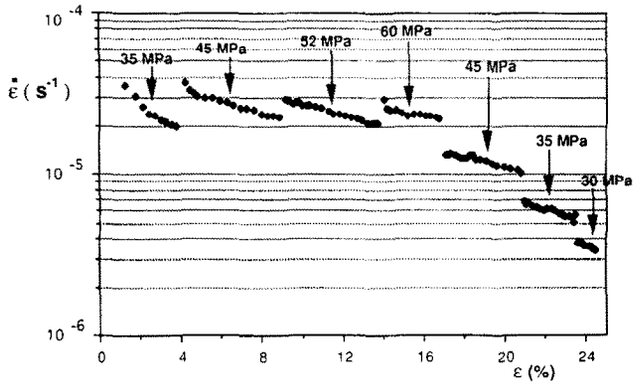

Fig. 5. Stress jumps from which the stress exponent n has been deduced (T = 1380°C).

Table 4. Average values of the stress exponent obtained at different stresses (T = 1380°C)

σ (*MPa*)	n	<n>
15→20→30→45	1·97	
35→45	1·94	1·95
45→60	1·55	
50→60	1·47	1·49
45→52→60	1·46	
60→72→86·4	1·72	
60→75→90	1·85	1·78

experimental average value <n> was slightly different from 2. It decreased down to nearly 1·5 for stressses ranging between 45 and 60 MPa, and then increased in the highest stress range studied (60–90 MPa).

3.5.3 Grain size exponent p

The strong effect of the grain size on the creep rate appeared clearly in all creep tests. The grain size exponent p has been determined directly by using eqn (2). To determine the initial creep rate corresponding to the initial grain size, the straight part of the $\ln\dot{\varepsilon}_S$ versus ε_S curves has been linearly extrapolated at zero strain. Under a stress of 60 MPa, its average value <p> was found to be 3 at 1380 and 1400°C.

4 Discussion

To test for the prospect of superplastic forming in the spinel system, polycrystalline samples of HIPed $MgO{\cdot}Al_2O_3$ spinel were deformed in compression at temperatures below 0·7 T_m. The following discussion is based on both the identification of the deformation mechanism and the determination of a possible way by which $MgO{\cdot}Al_2O_3$ spinel can be processed by superplastic forming.

This material presents a very good ability to be deformed to large strains because, after about 40% of true strain, no strain rate acceleration was observed. The absence of dislocation within the very fine-grained microstructure and the similarity of the equiaxed grain shapes before and after large creep flow resemble the features observed during microstructural superplasticity by diffusion-accommodated grain-boundary sliding.

Although the average values of the stress exponent (1·95 > n > 1·45) were similar to that obtained for superplasticity by diffusion-controlled dislocation climb by Panda *et al.*[12] in polycrystals of $MgO{\cdot}2Al_2O_3$ spinel (n = 2·1), we think that the present grain size dependence of the strain rate precludes dislocation motion as the origin of the rate-controlling mechanism. The variation of the average values of the stress exponent suggests a transition from n = 2 at low stresses to n approaching 1 at high stresses. This transition, with increasing stresses, needs to be considered within the concept of interface-controlled diffusional creep[22,23] in order to be understood. In fine-grained ceramics, interface reaction limitations of diffusional creep are more and more frequently observed. These limitations operate when the kinetics of mass transport depend not only on the rate-controlling diffusivities but also on the serial interface process by which grain boundaries act as sources or sinks for the vacancies. The non-linearity at low stresses can arise owing to energy barriers for the transfer of atoms across the interfaces.[24] The results of Sone *et al.*[16] substantiate this possibility of interface reaction control in superplastic deformation of fine-grained $MgO{\cdot}Al_2O_3$ spinel ceramic at 1380–1400°C, in the lowest part of the stress range studied (15–90 MPa).

In addition to being strongly dependent upon applied stress, the creep rate is observed to decrease linearly with strain. This can be attributed to the coupling between grain growth and the sliding mechanism of superplasticity. The value of the grain size exponent found at 60 MPa suggests that grain-boundary diffusion[21] makes a significant contribution at medium stresses to the diffusion-accommodated grain-boundary sliding.

Unfortunately it was not possible to obtain very large deformation without the generation of cavities. Since the cavitational creep mechanism in ceramics without an intergranular amorphous phase[25] yields a stress exponent n > 2, cavitational creep contribution was believed to be the cause of the lack of observation of purely Newtonian creep at stresses above 60 MPa. Because the extent of intergranular cavitation appeared to increase with increasing stress, only the stress range below 90 MPa has been explored. However, it has been possible to heal most of this damage by post-HIP

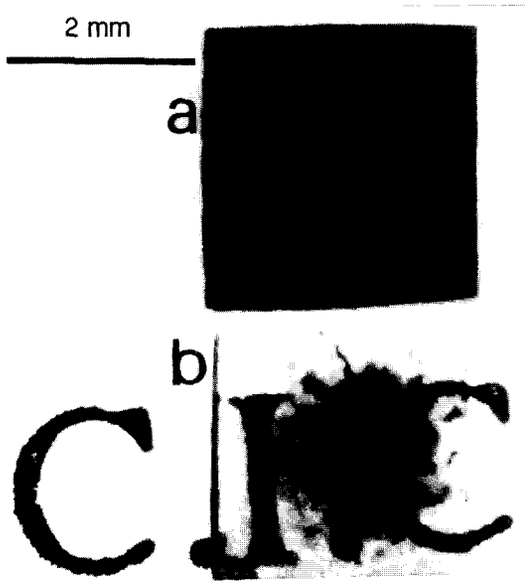

Fig. 6. Comparison between the transparency of (a) a deformed sample and (b) a post-HIPed sample.

treatment of the sample deformed at the lowest stresses (15–45 MPa).

Finally, the greatest impediment to the application of direct superplastic forming for perfectly dense $MgO{\cdot}Al_2O_3$ spinel ceramic is the presence, after processing, of these cavities, which interfere with the visible and i.r. transparency. However, post-HIP treatments realized to remedy this difficulty have shown that it is possible to improve the final density and then to restore some transparency, at least for parts superplastically deformed at temperatures below $0{\cdot}7T_m$ and at stress levels below ≈ 50 MPa. Figure 6 compares the sample deformed at the lowest stresses (15–45 MPa) and then post-HIPed with a sample that was deformed only. The final density level is close to the theoretical density and the transparency is improved except in the middle of the sample, where cavities still exist.

This result suggests a fabrication method in two steps for $MgO{\cdot}Al_2O_3$ spinel ceramic parts for optical applications. It consists of superplastic forging in open dies of nearly fully dense, presintered samples at temperatures below $0{\cdot}7T_m$, followed by a post-HIP treatment of superplastically forged parts, without a container, to increase the density and thus to improve the transparency.

5 Conclusion

Polycrystalline spinel of composition $MgO{\cdot}Al_2O_3$ was deformed in compression. Creep experiments performed from 15 to 90 MPa and from 1380 to 1400°C have shown that these polycrystals present a good ability to be superplastically deformed up to a true strain of about 40% with only a small density decrease.

Dynamic grain growth in the fine-grained matrix was very significant in our experiments, as it was in the case of several ceramics tested under various conditions of superplasticty.

In order to understand the variation of the average value of the stress exponent, suggesting a transition from $n = 2$ at low stresses to $n = 1$ at high stresses, the concept of interface-reaction-controlled diffusional creep must be invoked.

The grain size exponent was representative of grain-boundary sliding, probably accommodated by grain-boundary diffusion.

Superplastically deformed samples keeping their closed porosity stage were post-HIPed without a container. Post-HIP treatment results in a slight density increase and improved transparency for the sample deformed at the lowest stress. Accordingly, superplastic forging seems a potential option for near-net-shape forming of very fine-grained $MgO{\cdot}Al_2O_3$ spinel.

References

1. Chung, T. E. & Davies, T. J., The superplastic creep of uranium dioxide. *J. Nuclear Mater.*, **79** (1979) 143–153.
2. Crampon, J. & Escaig, B., Mechanical properties of fine-grained magnesium oxide at large compressive strains. *J. Am. Ceram. Soc.*, **63** (1980) 680–686.
3. Carry, C. & Mocellin, A., Superplastic forming of alumina. *Proc. Br. Ceram. Soc.*, **33** (1983) 101–115.
4. Wakai, F., Sakaguschi, S. & Matsumo, Y., Superplasticity of yttria-stabilized tetragonal ZrO_2 polycrystals. *Adv. Ceram. Mater.*, **1** (1986) 259–263.
5. Carry, C. & Mocellin, A., Structural superplasticity in single-phase crystalline ceramics. *Ceram. Int.*, **13** (1987) 89–98.
6. Gruffel, P., Carry, C. & Mocellin, A., Effect of testing conditions and doping on superplastic creep of alumina. *Rev. Phys. Appl.*, **23** (1988) 716–721.
7. Carry, C. & Mocellin, A., Examples of superplastic forming fine-grained Al_2O_3 and ZrO_2 ceramics. In *High Tech Ceramics, Materials Science Monograph 38A*, ed. P. Vincenzini. Elsevier Applied Science, Amsterdam, 1987.
8. Xu, X. & Chen, I. W., Superplastic bulging of fine-grained zirconia. *J. Am. Ceram. Soc.*, **73** (1990) 746–749.
9. Chen, I. W. & Xue, L. A., Development of superplastic structural ceramics. *J. Am. Ceram. Soc.*, **73** (1990) 2285–2609.
10. Becher, P. F., Press-forged Al_2O_3 spinel crystals for i.r. applications. *Am. Ceram. Soc. Bull.*, **56** (1977) 1015–1017.
11. Maguire, E. A. Jr & Gentilman, R. L., Press forging small domes of spinel. *Am. Ceram. Soc. Bull.*, **60** (1981) 255–256.
12. Panda, P. C., Raj, R. & Morgan, P. E. D., Superplastic deformation in fine-grained $MgO{\cdot}2Al_2O_3$ spinel. *J. Am. Ceram. Soc.*, **68** (1985) 522–529.
13. Panda, P. C. & Seydel, E. R., Near-net-shape forming of magnesia–alumina spinel/silicon carbide fiber composites. *Ceram. Soc. Bull.*, **65** (1986) 338–341.
14. Mitchell, T. E., Hwang, L. & Heuer, A. H., Deformation in spinel. *J. Mater. Sci.*, **11** (1976) 264–272.

15. Duclos, R., Doukhan, N. & Escaig, B., Study of the origin of the composition influence on the mechanical properties of $MgO{\cdot}nAl_2O_3$ spinels. *Acta Metall.*, **30** (1982) 1381–1388.
16. Sone, T., Akagi, H. & Takada, Y., Plastic deformation of fine-grained $MgAl_2O_4$ spinel ceramics. Abstract of the 94th Meeting of the Am. Ceram. Soc., Minneapolis, 1992.
17. Lappalainen, R., Pannikkat, A. & Raj, R., Superplastic flow in a non-stoichiometric ceramic: magnesium aluminate spinel. *Acta Metall. Mater.*, **41** (1993) 1229–1235.
18. Béclin, F., Duclos, R., Crampon, J. & Valin, F., Microstructural superplastic deformation in $MgO{\cdot}Al_2O_3$ spinel. *Acta Metall. Mater.*, **43** (1995) 2753–2760.
19. Ashby, M. F. & Verrall, R. A., Diffusion-accommodated flow and superplasticity. *Acta Metall.*, **21** (1973) 149–163.
20. Herring, C., Diffusional creep viscosity of a polycrystalline solid. *J. Appl. Phys.*, **21** (1950) 437–445.
21. Coble, R. L., A model for boundary diffusion controlled creep in polycrystalline materials. *J. Appl. Phys.*, **34** (1963) 1679–1684.
22. Burton, B., Interface reaction controlled diffusional creep: a consideration of grain boundary dislocation climb sources. *Mater. Sci. Eng.*, **10** (1972) 7–9.
23. Burton, B., The characteristic equation for superplastic flow. *Phil. Mag. A*, **48** (1983) L9–13.
24. Raj, R., Model for interface reaction control in superplastic deformation of non-stoichiometric ceramics. *Mater. Sci. Eng.*, **A166** (1993) 89–95.
25. Evans, A. G. & Rana, A., High temperature failure mechanisms in ceramics. *Acta Metall.*, **28** (1980) 129–141.